Directional Density of Gases Under FitzGerald-Lorentz Contraction: Predictions for Optical Interferometry

Alvydas Jakeliunas
Klaipėda, Lithuania
alvydas.jakeliunas@gmail.com
ORCID: 0009-0004-7265-1387

Abstract

We show that the directional density of an ideal gas remains isotropic under FitzGerald-Lorentz contraction of its container, while that of a bound solid becomes anisotropic. Combined with the invariance of the optical phase delay per molecule, this yields parameter-free predictions for gas-filled interferometers under Lorentzian Relativity. For a gas cell of physical length L measured against a direction-independent reference, the peak-to-peak fringe shift on a full rotation is $\Delta N = k\,(L/2\lambda)\,(n-1)\,(v/c)^2$, where k is the number of passes through the gas ($k = 1$ for a single pass, $k = 2$ for a round trip). The signal arises from the orientation-dependent molecule count in the contracted gas path. We predict null results for solid-dielectric interferometers regardless of refractive index.

1 Introduction

Special Relativity (SR) and Lorentz Ether Theory (LET) are kinematically equivalent for all phenomena involving bound systems. This equivalence is not accidental: it rests on the FitzGerald-Lorentz "conspiracy," in which length contraction, time dilation, and the electromagnetic response of bound matter combine precisely so as to render all optical path lengths direction-independent in any inertial frame. The null results of Michelson-Morley-type experiments using solid optical components — most recently, rotating fused-silica cavity experiments reaching $\Delta c/c \sim 10^{-17}$ [4, 5] — are the experimental expression of this conspiracy.

The conspiracy, however, has a logical prerequisite: the medium must *deform with the apparatus*. Bound matter satisfies this condition by definition — its constituents follow the lattice deformation. The question that motivates the present work is: what happens when this prerequisite fails? An ideal gas, whose molecules move freely and redistribute uniformly in any available volume, does not deform with the container in the same sense. It fills the contracted volume, but its spatial distribution remains isotropic — insensitive to the direction of contraction. This is a qualitative, not quantitative, departure from the bound-system case.

We show that this distinction has direct, observable consequences. The directional density — the number of molecules per unit length along a given direction — is isotropic for a gas and anisotropic for a solid under the same FitzGerald-Lorentz contraction. Combined with the frame-independence of the optical phase delay per molecule, this yields parameter-free predictions for gas-filled interferometers: a pure second-harmonic fringe shift on rotation, with amplitude $\Delta N = k\,(L/2\lambda)\,(n-1)\,\beta^2$, and a null result for solid-dielectric interferometers. The two predictions are not merely quantitatively different — they reflect a structural difference between SR and LET that is invisible in the bound-matter sector but becomes experimentally accessible through the thermodynamic properties of gases.

2 Directional Density

We define directional density $\rho_d(\hat{n})$ as the number of atoms per unit length along direction $\hat{n}$. For a homogeneous medium with uniform number density, directional density is the same in all directions.

Bound systems. In a crystal moving at velocity v, FitzGerald-Lorentz contraction compresses lattice spacings along $\mathbf{v}$ by a factor $1/\gamma$ while leaving perpendicular spacings unchanged. The directional density along $\mathbf{v}$ increases by γ; perpendicular directions are unaffected. Atoms cannot redistribute — they are held by binding forces. The anisotropy is $\Delta\rho_d/\rho_d \approx \beta^2/2$.

Unbound systems. When a gas container undergoes FitzGerald-Lorentz contraction along $\mathbf{v}$, the enclosed volume decreases to V/γ (contraction is a linear transformation with Jacobian $1/\gamma$). Gas, having no shear modulus and no shape memory, fills whatever volume is available uniformly. The 3D number density is therefore $N/(V/\gamma) = \gamma N/V$, isotropic and independent of container orientation. Crucially, when the container is rotated, the contracted volume remains V/γ — only the shape changes. A container aligned with $\mathbf{v}$ is shorter and wider; rotated 90°, it is longer and narrower; in both cases the enclosed volume is the same. The directional density therefore remains the same in all directions (Fig. 1).

The isotropy of the gas density distribution can be established by two complementary arguments. First, consider a mirror placed at 45° to $\mathbf{v}$ inside the gas. If molecules arrived more frequently from one direction than another, the mirror would generate a net macroscopic flow — violating thermodynamic equilibrium and, in principle, enabling a perpetual motion machine. Since no such flow exists, molecules must arrive at the mirror with equal frequency from all directions, regardless of the orientation of $\mathbf{v}$. This rules out any large anisotropy.

Second, within LET the mass of a molecule depends on its absolute speed relative to the ether. A molecule moving parallel to $\mathbf{v}$ at thermal speed v has ether-frame speed $w \pm v$, while one moving perpendicular has speed $\sqrt{w^2 + v^2}$. The linear number density along each direction is proportional to the corresponding Lorentz factor γ. Computing the ratio of the total density along $\mathbf{v}$ to that perpendicular to $\mathbf{v}$ gives:

$$\frac{\rho_\parallel}{\rho_\perp} - 1 \approx \tfrac{3}{2}\,\beta_w^2\,\beta_v^2 \tag{1}$$

where $\beta_w = w/c$ and $\beta_v = v/c$. For air at room temperature ($\beta_v \approx 1.7\times10^{-6}$) and $w \sim 300$ km/s ($\beta_w \approx 10^{-3}$), this gives a residual anisotropy of order 10^{-18} — twelve orders of magnitude below the predicted signal $\Delta N \propto \beta_w^2 \sim 10^{-6}$, and entirely negligible. The apparatus rotation and diffuse wall reflections provide additional mixing that further suppresses any residual anisotropy.

A solid, by contrast, deforms with the container: its atoms are bound to lattice sites and follow the shape change. The directional density of a crystal becomes anisotropic under contraction.

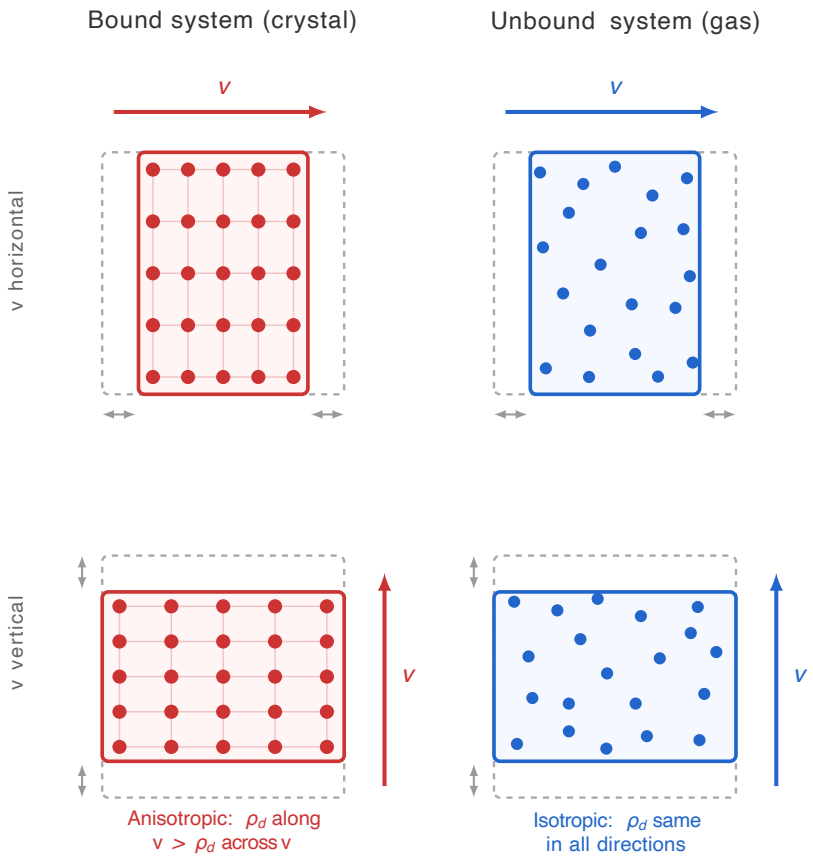

Figure 1: Directional density under FitzGerald-Lorentz contraction for two orientations of the velocity $\mathbf{v}$. Left column: crystal (bound) — atoms follow lattice deformation, directional density becomes anisotropic along $\mathbf{v}$. Right column: gas (unbound) — molecules redistribute uniformly in the contracted volume, directional density remains isotropic regardless of contraction direction. Dashed outline: rest-frame dimensions. Colored outline: contracted container.

3 Optical Phase in a Gas Path

The phase delay contributed by each gas molecule to a traversing photon is a Lorentz scalar $\delta\phi$ — it results from the electromagnetic interaction within a bound system (the molecule) and is frame-independent.[1] The total gas-induced phase along the beam path is:

$$\Phi_{\text{gas}} = N_{\text{path}} \times \delta\phi \tag{2}$$

where N_{path} is the number of molecules in the beam path.

A vacuum path, or a path through a solid medium (optical fiber, glass rod), serves as a reference. Being a bound system, it contracts with the apparatus, and its optical phase is direction-independent — this is the standard null result of vacuum interferometry.

[1]The phase delay per molecule can be derived by decomposing the photon transit into free propagation (at speed c) and interaction with the bound molecular system (Lorentz-transformed from the molecule's rest frame). The exact Fresnel drag coefficient emerges naturally from this decomposition, confirming its validity as a calculational tool without requiring a specific physical model of ether drag.

4 Interferometric Signal

Consider a gas cell of physical length L (measured with a ruler at rest) mounted alongside a vacuum reference channel on a rotating platform. As the platform turns, both channels sweep all directions in the horizontal plane.

Three interferometric configurations are natural candidates for testing the prediction. (i) A single-pass Mach-Zehnder interferometer with parallel gas and vacuum paths, as employed by Manley [2,3]. (ii) A reflected (round-trip) Mach-Zehnder or parallel-arm Michelson, in which end mirrors send the beams back through the same paths, doubling the signal ($k = 2$). (iii) Two parallel Fabry-Perot cavities on a common rotating platform — one evacuated, one gas-filled — with lasers locked to their respective resonances and the beat frequency monitored during rotation; this is the minimal modification to existing rotating-cavity apparatus [5,6]. Each configuration has its own balance of signal strength, systematic control, and experimental complexity.

The vacuum channel provides a direction-independent phase reference — its optical phase is the standard null result of bound-system interferometry.

The gas channel, oriented at angle θ to $\mathbf{v}$, has contracted length $L(\theta) = L(1 - \beta^2 \cos^2\theta/2)$. Since the gas density is isotropic and constant (Section 1), the molecule count in the beam path is simply proportional to the path length:

$$N(\theta) = N_0\left(1 - \frac{\beta^2 \cos^2\theta}{2}\right) \tag{3}$$

where N_0 is the rest-frame molecule count along the cell. The path contracts — fewer molecules fit along it. The formula is the same as for length contraction, applied directly to molecule count.

From molecule count to fringe shift. The total gas-induced phase delay (in wavelengths) for a single pass through the cell is $N_0 \times \delta\phi/(2\pi) = L(n-1)/\lambda$ (this is simply the well-known excess optical path $(n-1)L$ divided by λ). The variation in molecule count on rotation (Eq. 3) modulates this phase. Writing $\cos^2\theta = \frac{1}{2}(1 + \cos 2\theta)$, the peak-to-peak amplitude of the $\cos 2\theta$ oscillation in $N(\theta)$ is $N_0\beta^2/2$. Multiplying by the phase per molecule gives the single-pass fringe shift amplitude:

$$\Delta N_{\text{single}} = \frac{L}{2\lambda}(n-1)\beta^2 \tag{4a}$$

For a bidirectional (two-pass) configuration the photon traverses the gas cell twice, doubling the signal:

$$\Delta N_{\text{two-pass}} = \frac{L}{\lambda}(n-1)\beta^2 \tag{4b}$$

In compact notation: $\Delta N = k\,(L/2\lambda)\,(n-1)\,\beta^2$, where k is the number of passes through the gas ($k = 1$ single, $k = 2$ reflected). This is a parameter-free prediction: L and λ are apparatus constants, n is the measured refractive index, and v (hence β) is the velocity to be determined.

Numerical examples for air ($n - 1 = 2.73 \times 10^{-4}$ at 1 atm), gas cell length $L = 1$ m, $\lambda = 532$ nm, two-pass ($k = 2$):

	v (km/s)	β^2	ΔN
Galactic orbit (Cygnus)	220	5.4×10^{-7}	2.7×10^{-4} λ
CMB dipole (Leo)	370	1.5×10^{-6}	7.7×10^{-4} λ
At 10 atm ($n - 1 = 2.73 \times 10^{-3}$):			
Galactic orbit (Cygnus)	220	5.4×10^{-7}	2.7×10^{-3} λ
CMB dipole (Leo)	370	1.5×10^{-6}	7.7×10^{-3} λ

The signal scales linearly with gas pressure (through $n-1$), with cell length L, and with the number of passes k, offering direct routes to better sensitivity.

Harmonic content. If the velocity vector $\mathbf{v}$ makes angle ψ with the horizontal plane, the horizontal projection of the contraction is reduced by $\cos^2\psi$. The signal on rotation remains a pure second harmonic:

$$\Delta N(\theta) \propto \cos^2\psi \times \cos\, 2(\theta - \varphi) \tag{5}$$

where φ is the azimuthal direction of $\mathbf{v}$ projected onto the horizontal. The elevation ψ modulates the amplitude but does not change the harmonic order. A first-harmonic ($\cos\theta$) component in a horizontal interferometer therefore cannot arise from the directional density mechanism described here. Its presence may indicate systematic effects, or it may have an independent physical origin — for example, a directional interaction between the gas and a cosmic particle flow such as the dark matter wind (see Discussion). In configurations where the gas and vacuum paths are spatially separated by a distance d, the enclosed area $A = Ld$ makes the interferometer sensitive to the Sagnac effect from the platform rotation itself; sub-percent variations in the angular velocity over one turn then produce a first-harmonic signal that can mimic a physical effect. Regardless of its source, a first-harmonic signal is automatically suppressed in any bidirectional (two-pass) configuration, because any direction-dependent perturbation that slows light in the forward direction by δ speeds it by δ on the return, canceling to first order. This makes the two-pass geometry the preferred choice for isolating the second-order directional density signal.

However, if the gas cell is tilted at angle h relative to the rotation plane — for example, to sample a wider range of sky directions — the contraction factor $\cos^2\theta$ in Eq. (3) is evaluated along the tilted beam axis rather than in the horizontal plane. Decomposing $(\hat{n}\cdot\hat{v})^2$ for a beam tilted at angle h and velocity elevation ψ gives both a second-harmonic component (amplitude $\propto \cos^2 h\cos^2\psi$) and a first-harmonic component (amplitude $\propto \sin 2h \sin 2\psi$). Their ratio is $4\tan h\tan\psi$. This has two consequences: (i) the first harmonic vanishes when either $h = 0$ (no tilt) or $\psi = 0$ (velocity in horizontal plane), and (ii) even a moderate tilt can produce a large first harmonic when ψ is large — for example, at $h = 10°$ and $\psi = 48°$ (Cygnus from mid-latitudes) the ratio is already $\sim$0.8. Data taken at different tilt angles must be analyzed separately, and the harmonic content itself becomes a diagnostic of the geometry.

5 Predictions Across States of Matter

The analysis yields clean predictions for two limiting cases and an intermediate one.

Gases (unbound). Any gas whose molecules move freely — that is, not trapped by external electric or magnetic fields — qualifies as an unbound system. Molecules redistribute uniformly in the contracted volume, directional density remains isotropic, and the full signal $\Delta N = k\,(L/2\lambda)\,(n-1)\,\beta^2$ is predicted. This applies equally to air, helium, CO_2, or any other gas at any pressure.

Solids (bound). Atoms in a crystal or amorphous solid are locked to their equilibrium positions by binding forces. When the solid contracts, its atoms follow the deformation and the directional density becomes anisotropic. However, the optical response per unit cell transforms correspondingly — this is the FitzGerald-Lorentz "conspiracy," in which length contraction, time dilation, and the electromagnetic response of bound matter combine to render the optical phase direction-independent. Predicted signal: zero. This holds for any solid dielectric regardless of refractive index, consistent with the null results of modern rotating-cavity experiments using fused silica resonators [5,6].

Liquids (intermediate). Molecules in a liquid are mobile but interact strongly, with short-range order and characteristic relaxation times. Whether they redistribute fully (as in a gas) or partially follow the container deformation (as in a solid) depends on the balance between intermolecular forces and molecular mobility. Quantitative predictions for liquids require molecular dynamics simulations beyond the scope of this work.

The most unambiguous experimental test is therefore the comparison of a gas-filled interferometer (full signal predicted) with a vacuum or solid-reference interferometer (null predicted). The gas-versus-vacuum comparison involves no intermediate states and no modelling assumptions beyond ideal gas statistics.

6 Discussion

The signal in gas-filled interferometers arises from a counting asymmetry: a contracted arm contains fewer gas molecules than an uncontracted one, because gas redistributes isotropically while the arm does not. No vacuum condensate or ether drag model is invoked — only FitzGerald-Lorentz contraction and ideal gas statistics.

The prediction $\Delta N = k\,(L/2\lambda)\,(n-1)\,\beta^2$ coincides with the formula obtained by Consoli and Pluchino [1] through an independent analysis based on the non-trivial vacuum structure of quantum field theory. That two different approaches — one from statistical mechanics, one from vacuum condensate physics — yield the same functional dependence on $(n-1)$ and β^2 supports the validity of both results.

Manley [2,3] developed a rotating Mach-Zehnder interferometer comparing light propagation in gas and vacuum in parallel adjacent paths — a design well suited for testing these predictions. In his analysis[2], the combined signal amplitude is interpreted as a first-order effect ($\Delta N \propto v/c$), yielding an inferred velocity of $\sim$0.17 km/s. We were unable, however, to identify a physical mechanism by which the laboratory velocity $\mathbf{v}$ could produce a first-harmonic ($\cos\theta$) signal of the observed magnitude in a gas-filled interferometer; the directional density effect is strictly second order. We therefore focus on the second harmonic, which is the component predicted by the present analysis and whose amplitude is in good agreement with the formula of Consoli and Pluchino [1].

The dominant first-harmonic signal in Manley's data may have an independent origin unrelated to FitzGerald-Lorentz contraction. The fact that its celestial direction (RA $\approx$ 21.9 h, Dec $\approx +46°$) is broadly consistent with the dark matter wind toward Cygnus [7] — rather than the CMB dipole — is suggestive. A directional interaction between atmospheric gas molecules

[2]Manley, S.W.W. (2025). Unpublished preprint, viXra:2411.0125v1.

and a cosmic particle flow would produce a $\cos\theta$ dependence on rotation, since such an interaction distinguishes "toward" from "away." However, in a bidirectional (two-pass) configuration, any first-order directional perturbation cancels: light traveling forward and backward through the same gas accumulates equal and opposite shifts, leaving only even-order effects. The single-pass Mach-Zehnder geometry used by Manley does not benefit from this cancellation — which may explain why the first harmonic is prominent in his data. A reflected-beam geometry should suppress the first harmonic regardless of its origin and yield a clean second-harmonic signal amenable to the quantitative test described here.

Reading the second-harmonic amplitude from the data in [3] (approximately 0.2–0.3 in units of $\lambda/1000$, peak-to-peak) and applying the single-pass formula (Eq. 4a) $\Delta N = (L/2\lambda)(n-1)\beta^2\cos^2\psi$ with Manley's parameters ($L = 0.53$ m, $\lambda = 532$ nm, $n - 1 = 2.73 \times 10^{-4}$) gives an inferred velocity in the range 200–400 km/s, depending on the geometric projection factor $\cos^2\psi$. Two cosmic velocities fall in this range: the solar orbital velocity about the Galactic center ($\sim$220 km/s, apex toward Cygnus) and the motion of the solar system relative to the CMB rest frame ($\sim$370 km/s, apex toward Leo). The data in [3] do not yet distinguish between these candidates; a dedicated experiment with pressure scaling and diurnal tracking of the preferred direction would be needed to do so. The inferred velocity ($\sim$220 km/s) and direction (Cygnus) are notably consistent with the expected dark matter wind arising from the Sun's orbit through the Galactic dark matter halo [7]. If confirmed by a dedicated experiment, this would constitute a direct laboratory detection of the local dark matter rest frame — complementary to the particle-scattering searches currently pursued in underground experiments.

In any of the configurations described in Section 3, pressure variation provides a built-in calibration: the signal should scale linearly with gas pressure through $n - 1$. Comparing signals at several pressures — easily achieved with a roughing pump — would confirm or exclude the directional density mechanism independently of absolute amplitude.

The decisive experimental test is a comparison of interferometric signals in gas versus vacuum (or solid) reference paths, using a bidirectional (two-pass) beam geometry to suppress first-harmonic contamination. Two experimental configurations are recommended:

(1) Gas-filled Michelson interferometer on a rotating platform. Since the vacuum reference path is direction-independent by construction, both arms can be oriented parallel rather than perpendicular — the vacuum channel simply provides a stable phase reference against which the gas channel is measured. The preferred implementation (Fig. 2) places both channels in a single rigid block: one bore gas-filled at pressure p, the other evacuated. A beam splitter divides the laser into two beams entering the parallel channels; end mirrors reflects both beams back through the same paths (two-pass, $k = 2$). In this reflected-beam geometry, light traverses each channel in both directions, automatically canceling all first-order directional effects — whether from ether kinematics, dark matter interactions, or thermal gradients. Only the second-order directional density signal survives: a pure second harmonic $\Delta N = (L/\lambda)(n-1)\beta^2$. Stacking the two channels vertically (separation $d \to 0$) minimizes the enclosed area $A = Ld$, thereby suppressing the Sagnac phase shift that would otherwise arise from imperfect stabilization of the platform's angular velocity during continuous rotation. Pressure variation provides a built-in calibration: the signal should scale linearly with gas pressure through $n - 1$.

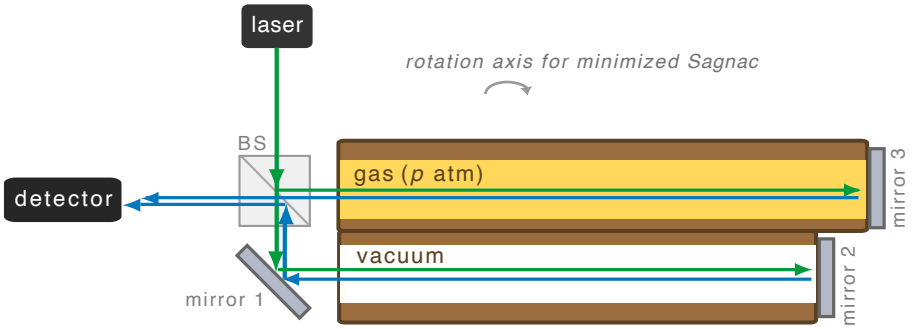

Figure 2: Recommended parallel-arm Michelson configuration. Two channels in a single rigid block — one gas-filled at pressure p, one evacuated — with end mirrors providing the two-pass geometry ($k = 2$). Green arrows: forward beam; blue arrows: return beam. Channels are stacked vertically to minimize the enclosed area $A = Ld$ and suppress the Sagnac effect from rotation speed fluctuations.

(2) Modified rotating optical cavity with gas cell. Modern rotating optical cavity experiments — which compare resonance frequencies of fused silica resonators on precision turntables — have reached sensitivities of $\Delta c/c \sim 10^{-17}$ and report null results [5,6]. Since these experiments use solid dielectrics, a null is exactly what the present analysis predicts (Section 4). The same apparatus, modified to include a gas-filled optical path, would have more than sufficient sensitivity to detect the predicted signal of order $(n-1)\beta^2 \sim 10^{-10}$ for air at atmospheric pressure — a margin of seven orders of magnitude. A gas-filled cavity will not achieve the same sensitivity as the solid reference: pressure and temperature fluctuations, molecular scattering losses, and reduced finesse will degrade performance by several orders of magnitude. Nevertheless, the predicted signal leaves ample margin even with substantially degraded sensitivity. The Fabry-Pérot cavities used in these experiments are inherently multi-pass configurations, providing the same first-harmonic suppression as the Michelson geometry.

Both configurations share two key advantages: (i) the bidirectional beam geometry eliminates first-harmonic signals from any source, and (ii) pressure variation offers a model-independent calibration, since the predicted signal scales linearly with $(n-1)$ while most systematic effects do not. Increasing the gas pressure to 10 atm raises the signal to $\sim 10^{-9}$, further simplifying detection.

Acknowledgements

The author thanks Victor O. de Haan for years of discussions on ether theories and optical interferometry, and for sharing his experimental insights that have shaped the ideas presented here.

Statements and Declarations

Funding. The author received no external funding for this research.

Competing interests. The author has no competing interests to declare that are relevant to the content of this article.

Data availability. No datasets were generated or analysed during the current study. All quantitative results follow analytically from the formulae presented, which are reproducible from the equations in this article. The article is archived at `https://zenodo.org/records/18824161`.

Author contributions. A.J.: conceptualization, formal analysis, writing – original draft, writing – review & editing.

References

[1] Consoli, M. & Pluchino, A. (2023). Int. J. Mod. Phys. A **38**, 2330017. `https://doi.org/10.1142/S0217751X2330017X`

[2] Manley, S.W.W. (2023). Eur. Phys. J. Plus **138**, 206. `https://doi.org/10.1140/epjp/s13360-023-03812-w`

[3] Manley, S.W.W. (2024). Eur. Phys. J. Plus **139**, 730. `https://doi.org/10.1140/epjp/s13360-024-05529-w`

[4] Herrmann, S. et al. (2009). Phys. Rev. D **80**, 105011. `https://doi.org/10.1103/PhysRevD.80.105011`

[5] Eisele, Ch., Nevsky, A. Yu. & Schiller, S. (2009). Phys. Rev. Lett. **103**, 090401. `https://doi.org/10.1103/PhysRevLett.103.090401`

[6] Freese, K., Lisanti, M. & Savage, C. (2013). Rev. Mod. Phys. **85**, 1561. `https://doi.org/10.1103/RevModPhys.85.1561`